

**TECHNISCHE  
UNIVERSITÄT  
DRESDEN**

---

# Investigation of nonhyperbolic dynamical systems

Bachelor-Arbeit  
zur Erlangung des Hochschulgrades  
Bachelor of Science  
im Bachelor-Studiengang Physik

vorgelegt von

**FELIX SCHAUMANN**

geboren am 27.09.1996 in LANDSBERG AM LECH

Max-Planck-Institut für Physik komplexer Systeme  
Fakultät Physik  
Bereich Mathematik und Naturwissenschaften  
Technische Universität Dresden  
2019

Eingereicht am 04. Juni 2019

1. Gutachter: Prof. Dr. Holger Kantz
2. Gutachter: Prof. Dr. Marc Timme

---

## ABSTRACT

The aim of this thesis is to analyze the effect of nonhyperbolicity on a nonlinear dynamical system. The focus lies on the distribution of periodic points on the attractor. Since unstable periodic orbits are the basis for many calculations in dynamical systems theory, their distribution is of special importance.

Two systems are regarded in this thesis: the nonhyperbolic Hénon map and the hyperbolic dissipative baker map. For both systems, the unstable periodic orbits and other important quantities are calculated. Starting from a qualitative approach, the presence and location of parts of the Hénon attractor without periodic points and their dependence on the period length is discussed. Later, quantitative tools for analyzing the distribution of periodic points on the attractor are developed and applied to the Hénon map.

Finally, an explanation for the observed gaps on the Hénon attractor is sketched, connecting them to generating partitions and symbolic dynamics.

## ZUSAMMENFASSUNG

Das Ziel dieser Arbeit ist es, die Auswirkungen der Nichthyperbolizität auf ein dynamisches System zu untersuchen. Das Augenmerk liegt hierbei auf der Verteilung der periodischen Punkte auf dem Attraktor. Da instabile periodische Orbits die Grundlage für viele Berechnungen in der Theorie dynamischer Systeme bilden, ist ihre Verteilung von besonderer Bedeutung.

In dieser Arbeit werden zwei Systeme betrachtet: die nichthyperbolische Hénon-Abbildung sowie die hyperbolische und dissipative Bäcker-Abbildung. Für beide Systeme werden die instabilen periodischen Orbits und andere wichtige Größen berechnet. Mit einer qualitativen Herangehensweise wird die Existenz und Lage von Bereichen des Hénon-Attraktors ohne periodische Punkte betrachtet, sowie deren Abhängigkeit von der Periodenlänge. Anschließend werden quantitative Methoden zur Analyse der Verteilung von periodischen Punkten auf dem Attraktor entwickelt und auf die Hénon-Abbildung angewendet.

Schließlich wird eine Erklärung skizziert, die die beobachteten Lücken im Hénon-Attraktor mit erzeugenden Partitionen und symbolischen Dynamiken verknüpft.



# Contents

<b>1</b>	<b>Introduction</b>	<b>1</b>
<b>2</b>	<b>Fundamentals</b>	<b>3</b>
2.1	Hyperbolicity and Homoclinic Tangencies . . . . .	3
2.2	Periodic Orbits and Axiom A systems . . . . .	4
2.3	Generating partitions and symbolic dynamics . . . . .	5
2.4	Hénon map and baker map . . . . .	6
<b>3</b>	<b>Calculations</b>	<b>9</b>
3.1	Unstable Periodic Orbits . . . . .	9
3.2	Stable and Unstable Manifolds . . . . .	12
3.3	Homoclinic Tangencies . . . . .	12
<b>4</b>	<b>Effects of Nonhyperbolicity</b>	<b>15</b>
4.1	Gaps around Homoclinic Tangencies . . . . .	15
4.2	Distribution of periodic points . . . . .	18
4.3	Origin of gaps in the Hénon attractor . . . . .	24
<b>5</b>	<b>Summary and Outlook</b>	<b>29</b>
<b>6</b>	<b>Bibliography</b>	<b>31</b>



# 1 Introduction

Complexity is a necessary feature of the living world. Neither life itself, nor the natural environment would be possible without the complex system of a biological cell. And most of the surrounding non-biological systems, such as the atmosphere, the oceans, cities or transport networks, are highly complex as well. It is therefore of central importance to develop quantifiable concepts for describing these systems.

Dynamical systems theory is such an approach. A dynamical system is a set of equations that can describe the state a system is in and handle its time evolution. They are used to model the behaviour of known complex systems and are the testing ground for quantitative methods that can later be applied to data from unknown systems.

Even very simple dynamical systems exhibit a phenomenon coined chaos: a very sensitive dependence of the result on the initial conditions. This places a practical limit to the calculability of such systems, since the initial conditions can only be known up to a certain precision. It is possible to model complex systems with a set of deterministic equations, thereby creating a phenomenon called deterministic chaos [1]. The time evolution of any initial state can be determined from the equations defining the system. Yet, since initially similar trajectories in phase space often diverge into completely different behaviour, it is necessary to develop tools that are able to capture the general properties of a system independent of a concrete choice of initial conditions.

A central quantity of a dynamical system is its natural measure, which assigns a probability of occurrence to any point in phase space. For an ergodic<sup>1</sup> system, this is equivalent to the normalized spatial distribution of a very long trajectory [1, 2]. The natural measure allows to determine the states, described by points in phase space, the system is most probable to be in.

Other important quantities are generalized dimensions, describing the dimensionality of the subset of phase space that is visited by the system in the long run, and entropies, which can be regarded as giving a measure for the complexity of the system [3, 4]. A related concept is that of Lyapunov exponents. They describe, for every dimension of the phase space, at which rates a small segment of phase space expands or contracts [5, 6, 7].

All these quantities describe the system as a whole, without looking at a particular trajectory with certain initial conditions. In practice, it can be quite hard to calculate these quantities,

---

<sup>1</sup>We will only treat ergodic systems in this thesis.

since it is necessary to find a typical set of trajectories that are able to represent the general properties of the dynamics and are invariant under coordinate change. The alternative approach is to use unstable periodic orbits [5, 8]. Periodic orbits are trajectories in phase space whose dynamics repeat after a certain amount of iterations. For many systems, the set of periodic points is countable, being finite for a given period length of the orbit. To calculate dimensions, measures or entropies, it is often sufficient to regard periodic orbits only up to a certain period length, since the result converges relatively fast. Being able to work with a finite set of points that is nonetheless representative for the dynamics as a whole, makes this method very effective.

Yet these results do not apply to all dynamical systems equally. They were proved for *hyperbolic* systems. [9], but most systems of interest are nonhyperbolic and thereby lack many important properties, such as structural stability [10]. It has been investigated to what extent the above stated results hold for *nonuniformly hyperbolic* systems [11, 12, 13, 14]. In [14], for example, it is shown that the natural measure can be approximated by periodic orbits for nonhyperbolic systems. But there are phenomena emerging in nonhyperbolic systems that indicate a structural difference from hyperbolic systems, such as the deviation of periodic orbits from the natural measure for low period lengths.

This thesis will tackle the effects of nonhyperbolicity on the distribution of periodic points. After introducing the basic definitions and concepts in Chapter 2, Chapter 3 describes how we calculate the periodic orbits of two representative systems, and the points of homoclinic tangency, a central feature of the nonhyperbolic Hénon map. In Chapter 4 we will have a look at the distribution of periodic orbits on the attractor, to discuss phenomena like gaps around homoclinic tangencies and deviations from the natural measure. Based on these investigations, an explanation for the origin of the observed gaps in the nonhyperbolic Hénon attractor is presented. Finally, in Chapter 5 the results are summarized and a brief outlook on possible directions for future investigations is given.



# 2 Fundamentals

## 2.1 Hyperbolicity and Homoclinic Tangencies

One of the most used concepts in the study of complex systems is local stability analysis.

The stability of a point  $\mathbf{x}_0$ <sup>1</sup> in phase space refers to whether, under successive iteration, points in near vicinity approach  $\mathbf{x}_0$  or diverge from it. To analyze the stability of a point, it is helpful to linearize the dynamics, i.e. to perform a Taylor expansion. We will follow [15] and [2] for this topic. This leads to the first important distinction, between continuous systems and discrete systems, called maps.<sup>2</sup> A continuous system is characterized by differential equations  $\frac{d\mathbf{x}}{dt} = \mathbf{f}(\mathbf{x})$ , a map by an iteration rule  $\mathbf{x}_n = \mathbf{f}^n(\mathbf{x}_0)$  [16].

If we regard a map  $\mathbf{f}$ , with  $\mathbf{x}_{n+1} = \mathbf{f}(\mathbf{x}_n)$ , the linear expansion around  $\mathbf{x}_0$  gives

$$\mathbf{f}(\mathbf{x}_0 + \delta\mathbf{x}) = \mathbf{f}(\mathbf{x}_0) + \mathbf{J}(\mathbf{x}_0) \delta\mathbf{x} + \dots, \quad (2.1)$$

where  $J_{ij} = \frac{\partial f_i}{\partial x_j}$  is the Jacobian. Obviously, the Jacobian can only be calculated if the map is differentiable. Equation 2.1 can transport a point in the local linearized neighborhood of  $\mathbf{x}_0$ , the tangent space  $T_{\mathbf{x}_0}$ . The eigenvectors of the Jacobian span different subspaces,  $E_{\mathbf{x}_0}^s$ ,  $E_{\mathbf{x}_0}^u$  and  $E_{\mathbf{x}_0}^c$ , called stable, unstable and center subspace [2]. For a negative eigenvalue, the corresponding eigenvector is in  $E_{\mathbf{x}_0}^s$ , for a positive eigenvalue in  $E_{\mathbf{x}_0}^u$  and for an eigenvalue  $\lambda_i = 0$  it is in  $E_u$ .

We call a point  $\mathbf{x}_0$  *hyperbolic* if its tangent space is spanned by the stable and the unstable subspace, i.e. if  $T_{\mathbf{x}_0} = E_{\mathbf{x}_0}^s \oplus E_{\mathbf{x}_0}^u$  [10]. A set  $\Lambda$  is called *hyperbolic* if every  $\mathbf{x}_0 \in \Lambda$  is hyperbolic. This is the case if (i) the center subspace  $E^c$  is of dimension zero and (ii) all eigenvectors of  $\mathbf{J}(\mathbf{x})$  are linearly independent for all  $\mathbf{x} \in \Lambda$ . In this thesis we will focus on the latter violation of hyperbolicity, which leads to nonhyperbolic systems with homoclinic tangencies.

We can now define the stable and unstable manifold.

The *stable manifold*  $W^s$  of a point  $\mathbf{x}$  is the set of points that approach  $\mathbf{x}$  under forward iteration, and it has the same dimensionality as the stable subspace around  $\mathbf{x}$ : [2]

$$W_{\mathbf{x}}^s = \{\mathbf{y} \mid \lim_{n \rightarrow \infty} \|\mathbf{f}^n \mathbf{y} - \mathbf{f}^n \mathbf{x}\| = 0\}, \quad \dim(W_{\mathbf{x}}^s) = \dim(E_{\mathbf{x}}^s) \quad (2.2)$$

---

<sup>1</sup>Throughout this thesis, bold letters will indicate vectors, and bold capital letters matrices.

<sup>2</sup>We will only regard maps in this thesis, since they are discrete and therefore easier to handle numerically.

Analogously, the *unstable manifold*  $W^u$  is the set of points that approach  $\mathbf{x}$  under backwards iteration: [10]

$$W_{\mathbf{x}}^u = \{\mathbf{y} \mid \lim_{n \rightarrow -\infty} \|\mathbf{f}^n \mathbf{y} - \mathbf{f}^n \mathbf{x}\| = 0\}, \quad \dim(W_{\mathbf{x}}^u) = \dim(E_{\mathbf{x}}^u) \quad (2.3)$$

A point  $\mathbf{x}$ , at which the stable manifold  $W_{\mathbf{x}}^s$  and the unstable manifold  $W_{\mathbf{x}}^u$  are tangential, is called a *homoclinic tangency (HT)*. Since the linear subspaces must in this case also be tangential, they can no longer span the whole phase space and  $\mathbf{x}$  is therefore not hyperbolic. HTs are the manifestation of nonhyperbolicity that we are interested in in this thesis.

## 2.2 Periodic Orbits and Axiom A systems

Periodic orbits are a central concept in dynamical systems theory, since they are the basis for calculating most characteristic quantities. An orbit is called periodic, if, after a certain amount of iterations, it maps back to itself. Every member of a  $p$ -periodic orbit is a fixed point of the  $p$ -th iterate of the map  $\mathbf{f}$ :

$$\mathbf{f}^p \mathbf{x} = \mathbf{x} \quad (2.4)$$

The solutions to equation 2.4 are finite for a fixed period length  $p$ , but  $p$  can be chosen arbitrarily large, which leads to an infinite number of periodic orbits. In practice, periodic orbits can only be calculated up to a certain period length  $P$ . One can therefore work with a finite set of periodic orbits of different lengths  $p \leq P$ .

An important distinction is that between conservative and dissipative systems. A conservative system is characterized by the conservation of energy, which translates into a conservation of phase space volume. A dissipative system has a shrinking phase space volume. Mostly, this leads to the presence of an attracting set, where most trajectories wander to, called an *attractor* [2]. It is a nonwandering set for a dissipative system, into which every point inside a bigger set, the basin of attraction, is eventually mapped. A subset of the phase space is called a *nonwandering set*, if it is the smallest possible set whose points are exclusively mapped back into the set itself. Consequently, whenever a point lies in the nonwandering set, it will stay inside it for any number of iterations.

An attractor can consist of a point, of a set of points or even be a fractal set. The latter is called a *strange attractor*. If every point of the attractor is hyperbolic, then it is a hyperbolic attractor. If there are points violating the hyperbolicity, we call it a nonuniformly hyperbolic attractor.

A special class of dynamical systems, introduced by Stephen Smale, are the Axiom A systems. They are defined by the following properties [8]:

- The nonwandering set of the system is hyperbolic.

- The set of periodic points of the system is dense in the nonwandering set.

If the nonwandering set is a hyperbolic attractor, it was actually proved that the second property follows from the first [17]. In this case, the distribution of the periodic points approaches the natural measure for increasing period length [8]. It is therefore interesting to investigate whether these very convenient properties of hyperbolic attractors can be expected to be valid for nonuniformly hyperbolic attractors, which are by definition not Axiom A.

## 2.3 Generating partitions and symbolic dynamics

An arbitrary initial condition of a system with a strange attractor will result in nonperiodic chaotic behaviour [2]. One way of characterizing this specific orbit, is to indicate the initial condition with high precision. Another is to determine, in which part of the phase space it lies for every iteration. This is done with the help of *generating partitions*. A generating partition (GP) is one that, together with all its images and preimages, subdivides the phase space into arbitrarily fine segments [18]. Generating partitions are essential for the calculation of quantities such as the Kolmogorov-Sinai entropy [19, 6]. For many two-dimensional systems<sup>3</sup>, binary generating partitions exist. This means that the phase space is divided into two parts by a partition line, and every point can be coded with a 1 or a 0, depending on the part it lies in. If we code a complete orbit with the respective partition element in which the iterated points lie, we get to the concept of *symbolic dynamics*. The dynamics of an orbit is coded with arbitrarily chosen symbols (in our case, since it is a binary partition, with 1 and 0). The symbolic dynamics consists of as many symbols as the orbit is long. Therefore, a nonperiodic orbit has a biinfinite symbolic dynamics, since it can be iterated infinitely many times both forwards and backwards. A  $p$ -periodic orbit has a symbolic dynamics which is periodic with period  $p$ , for example a infinite repetition of (000001) for period  $p = 6$ .

The concept of symbolic dynamics is very useful, since any orbit can be coded in a distinct way, at least for smooth invertible systems [2]. No two different orbits of an invertible system ever map to the exact same point, so they can always be distinguished by their initial condition. It is clear that a generating partition, dividing phase space into arbitrarily small segments, can in principle determine the starting point with arbitrary precision. Therefore every orbit has a unique symbolic dynamics. For periodic orbits, it is even finite, and very useful for calculations, as we will see in section 3.1.

---

<sup>3</sup>Including the two systems investigated in this thesis [18].

## 2.4 Hénon map and baker map

To study the properties of nonhyperbolic maps, we will investigate two systems, one that is hyperbolic and one that is not. The two systems studied in this thesis are the dissipative Hénon map (from now on just called Hénon map) and the dissipative baker map (from now on called baker map). Both are nonlinear two-dimensional maps.

The Hénon map is given by: [20]

$$\begin{pmatrix} x_{n+1} \\ y_{n+1} \end{pmatrix} = \begin{pmatrix} a + by_n - x_n^2 \\ x_n \end{pmatrix} \quad (2.5)$$

It can be useful to reduce the map to a one-dimensional form by substituting  $y_n = x_{n-1}$ . This gives

$$x_{n+1} = a + bx_{n-1} - x_n^2. \quad (2.6)$$

In this thesis, the two parameters will be the canonical choice [20]:  $a = 1.4$ ,  $b = 0.3$ . With this choice, the map has a strange attractor, as shown in Figure 2.1(a). The attractor has a fractal structure, caused by the mechanism of ‘stretching and folding’ [21, 20]. We note that the Hénon map is invertible.

The baker map, as we define it in this thesis, is given by:

$$\begin{pmatrix} x_{n+1} \\ y_{n+1} \end{pmatrix} = \begin{pmatrix} 2 \cdot x_n \\ \alpha \cdot y_n \end{pmatrix} + \Theta\left(x_n - \frac{1}{2}\right) \cdot \begin{pmatrix} -1 \\ \frac{1}{2} \end{pmatrix} \quad (2.7)$$

$\Theta(x)$  is the step function. The second term is nonzero only if  $x_n \geq \frac{1}{2}$ . The attractor of the baker map is shown in Figure 2.1(c). It exhibits a fractal structure in the y coordinate, as we can see from zooming in (Figure 2.1(d)). Since we want to compare the two systems as well as possible, we choose the parameter  $\alpha$  such that the Hausdorff dimension  $D_B$  of both attractors is equal. Following [1], for the baker map we get  $D_B = 1 + D_y = 1 + \frac{\ln 2}{|\ln \alpha|}$ . For more details, see [22, 3]. The Hausdorff dimension of the Hénon map with canonical parameters is  $D_B(a = 1.4, b = 0.3) = 1.26$  [1]. Therefore we set  $\alpha$  to  $\alpha = \exp\left(\frac{-\ln(2)}{0.26}\right) \approx 0.07$ .

The baker map is clearly hyperbolic, since it only contracts in y direction and the x values do not depend on the y direction. Therefore, we have a weakly, but steadily expanding x direction and a strongly contracting y direction, which are always orthogonal and span the whole phase space.

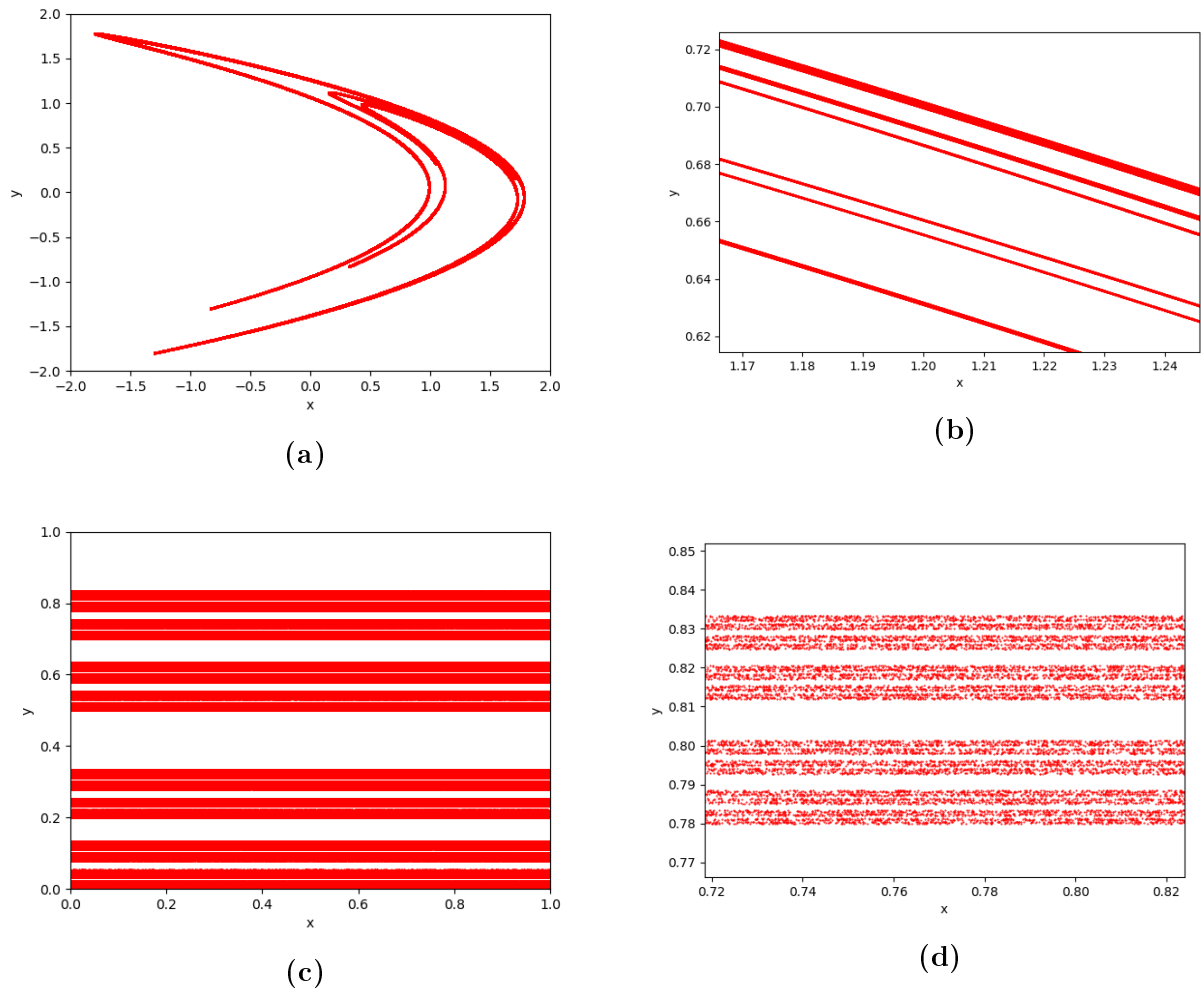


**Figure 2.1:** Attractors of the Hénon map in (a), zoomed in in (b) and of the baker map in (c), zoomed in in (d). For a better visualization of the baker map, we used  $\alpha = 0.4$  in this plot. A smaller  $\alpha$  would further compress the attractor in the y direction.



# 3 Calculations

## 3.1 Unstable Periodic Orbits

In principle, all unstable periodic orbits (UPOs) can be calculated. But the difficulty strongly depends on the map. For the baker map it is easy and computationally cheap, since it can be reduced to linear equations. For the Hénon map, Biham and Wenzel suggested an algorithm that allows the calculation of all UPOs of a certain period  $p$  [23]. They found a Hamiltonian, whose Euler-Lagrange equations are exactly the Hénon map. In this setting, extremum configurations of the Hamiltonian correspond to periodic orbits of the Hénon map, when applying periodic boundary conditions. Specifically, for period  $p$  and a set of  $p$  variables  $\mathbf{x}(t) = x_1(t), \dots, x_p(t)$  with  $x_{p+1} = x_1$ , the following differential equations are solved: [11]

$$dx_n/dt = s_n f_n(\mathbf{x}) \tag{3.1}$$

where  $s_n$  are constant factors and

$$f_n(\mathbf{x}) = x_{n+1} - a - bx_{n-1} + x_n^2. \tag{3.2}$$

The time  $t$  is an artificial coordinate that is introduced to lead the system to an extremum configuration. If there is a solution to the system of differential equations 3.1, then for big times  $t$  the state coordinate  $\mathbf{x}$  will be constant and, since  $s_n$  are constant as well,  $f_n(\mathbf{x})$  will be zero. It is easy to see in 3.2 that this case corresponds to a solution of the Hénon map.

Biham and Wenzel showed that it is sufficient to choose the constant factors as  $s_n = \pm 1$  [24]. They claimed that  $\{s_n\}$  gives a symbolic dynamics of the periodic orbit. For the canonical coordinates of the Hénon map this was verified in [11]. This results in a maximum of  $2^p$  solutions for a periodic orbit of length  $p$ . Actually, the number is lower than that, since not all binary sequences correspond to a solution.

One has to take into account that sometimes different binary sequences  $\{s_n\}$  can lead to the same orbit. This is the case for repetitions and for cyclic permutations. The sequence (100100)<sup>1</sup> is just a double run through the sequence (100) and can be discarded. All its information is contained in the shorter sequence. Since for a periodic orbit the starting point is irrelevant, (100010) is equivalent to (010001) and only one of each class of possible cyclic permutations

---

<sup>1</sup> $s_n = \pm 1$  can be coded by any two signs. Binary coding with 1 and 0 is convenient.

has to be regarded.

After having calculated the periodic orbits of the Hénon map up to a certain period length  $P = 21$ , one can check the result by calculating the topological entropy. The topological entropy can be understood as a measure for complexity of the regarded system. It measures, by which exponent the number of distinguishable orbits grows with the orbit length. It can be estimated on the basis of UPOs (see [11]) by

$$k = \lim_{p \rightarrow \infty} k_p \quad \text{with} \quad k_p = \frac{1}{p} \ln(N(p) - 1), \quad (3.3)$$

where  $p$  is the period length and  $N(p)$  the amount of periodic points at period length  $p$ . The  $k_p$  for the calculated period lengths can be seen in Figure 3.1. We see that they converge to a value around the previously calculated  $k = 0.465$  [11]. Although this result only accounts for the amount of calculated points and not for the correctness of their coordinates, it is a strong indicator that the Biham-Wenzel algorithm was implemented correctly.

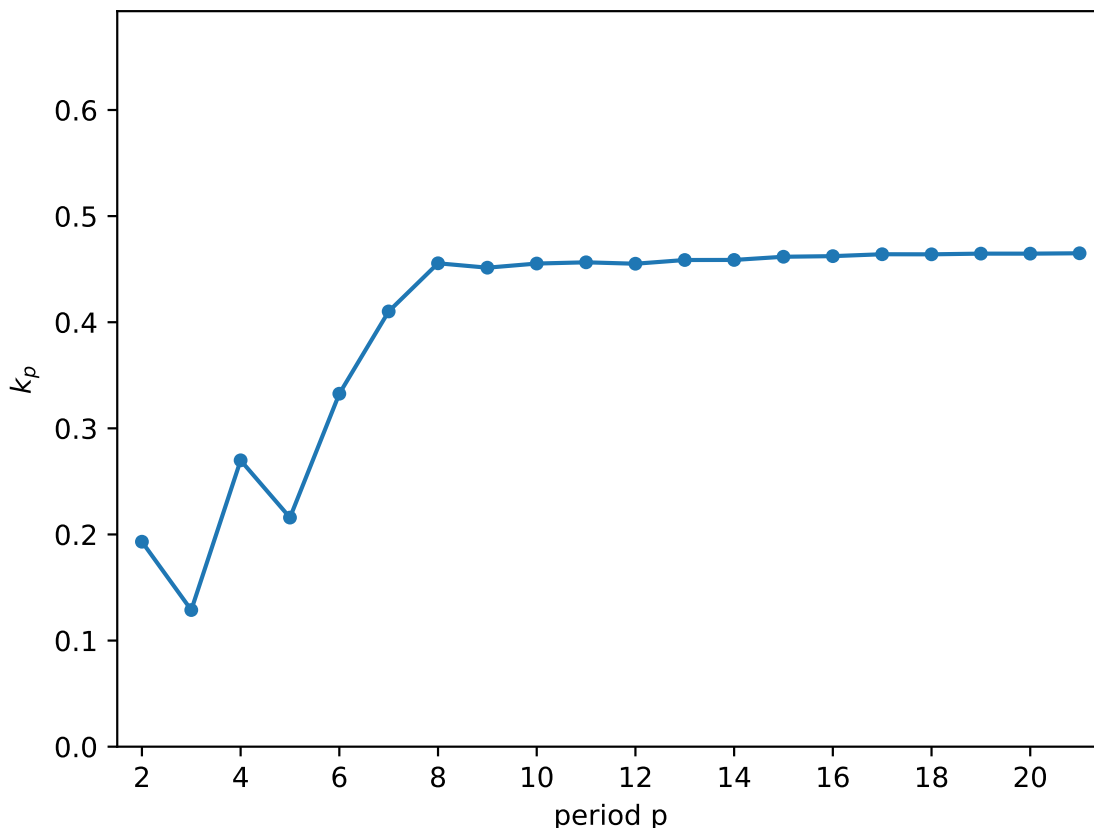


**Figure 3.1:** Topological entropy  $k_p$  of the Hénon map for different period lengths  $p$ .

Calculating the UPOs of the baker map is easy, since the x coordinate does not depend on the y coordinate. Therefore the periodic orbits of the x direction can be calculated first. Again, we



introduce symbolic dynamics. We can use the same binary sequences as for the Hénon map, with cyclic permutations and repetitions of lower-dimensional sequences excluded. Then, for the x coordinate, in order to get the periodic orbits corresponding to a symbol sequence  $\{s_n\}$ , we need to calculate

$$\begin{pmatrix} x_1 \\ x_2 \\ \vdots \\ x_p \end{pmatrix} = \begin{pmatrix} 0 & 0 & \cdots & 2 \\ 2 & 0 & \ddots & 0 \\ 0 & \ddots & \ddots & \vdots \\ \vdots & \ddots & 2 & 0 \end{pmatrix} \cdot \begin{pmatrix} x_1 \\ x_2 \\ \vdots \\ x_p \end{pmatrix} - \begin{pmatrix} s_1 \\ s_2 \\ \vdots \\ s_p \end{pmatrix}, \quad (3.4)$$

where  $s_n$  are the symbols of the binary sequence, when using 0 for  $x_{n-1} < \frac{1}{2}$  and 1 for  $x_{n-1} \geq \frac{1}{2}$ . It is easy to verify that for a UPO of period  $p$  the x coordinates of the periodic points are  $x_i = \frac{i}{2^p-1}$ , with  $i \in \{0, \dots, 2^p - 1\}$ .

To calculate the y coordinates, we apply the same procedure and need to calculate

$$\begin{pmatrix} y_1 \\ y_2 \\ \vdots \\ y_p \end{pmatrix} = \begin{pmatrix} 0 & 0 & \cdots & \alpha \\ \alpha & 0 & \ddots & 0 \\ 0 & \ddots & \ddots & \vdots \\ \vdots & \ddots & \alpha & 0 \end{pmatrix} \cdot \begin{pmatrix} y_1 \\ y_2 \\ \vdots \\ y_p \end{pmatrix} + \frac{1}{2} \cdot \begin{pmatrix} s_1 \\ s_2 \\ \vdots \\ s_p \end{pmatrix}, \quad (3.5)$$

The x and y trajectories calculated for the same symbol sequence, as both coordinates only depend on the previous x coordinate, together give the trajectory  $(x_n, y_n)$  of a UPO. We note that, in contrast to the Hénon map, every symbol sequence yields an existing orbit, since the linear equations to be solved all have existing solutions.

## 3.2 Stable and Unstable Manifolds

The stable and the unstable manifold at  $\mathbf{x}_0$  can be approximated locally by calculating the direction with the strongest expansion and that with the strongest contraction.

We first compute an iterate of the Hénon map of length  $I = 10^5$  and save the coordinates of the points. Starting with an arbitrary vector  $\mathbf{v}_0^u$  of norm  $\|\mathbf{v}_0^u\| = 1$ , we calculate iteratively

$$\mathbf{v}_{i+1}^u = \frac{\mathbf{J}(\mathbf{x}_{i+1}) \cdot \mathbf{v}_i^u}{\|\mathbf{J}(\mathbf{x}_{i+1}) \cdot \mathbf{v}_i^u\|}, \quad (3.6)$$

with  $\mathbf{x}_i$  being the points of the previously calculated chaotic orbit. As in equation 2.1, the Jacobian bends the vector into the direction with the strongest expansion. The other directions are suppressed by the normalization. Since the Hénon attractor is ergodic, with a sufficiently long orbit every part of it is covered. For every regarded point  $\mathbf{x}_i$  we obtain the direction with the strongest expansion rate, given by the vector  $\mathbf{v}_i^u$ .<sup>2</sup>

Inverting the Jacobian, we can compute the stable manifold on the attractor by performing the same calculation backwards, starting from  $\mathbf{x}_I$ .

$$\mathbf{v}_{i-1}^s = \frac{\mathbf{J}^{-1}(\mathbf{x}_{i-1}) \cdot \mathbf{v}_i^s}{\|\mathbf{J}^{-1}(\mathbf{x}_{i-1}) \cdot \mathbf{v}_i^s\|}, \quad (3.7)$$

Figure 3.2 shows both vector fields. We see that the unstable manifold is always tangential to the attractor and the stable manifold is mostly normal to the attractor. There are however regions in phase space in which the stable manifold is also tangential to it, and thereby also tangential to the unstable manifold. These are the regions of homoclinic tangencies (HTs), which are of great importance to this work, since they determine the nonhyperbolicity of the Hénon map.

## 3.3 Homoclinic Tangencies

We calculate the HTs by comparing the stable and the unstable vector for every regarded point  $\mathbf{x}_i$  on the attractor. If they are sufficiently parallel, i.e. if their dot product surpasses a certain threshold  $\gamma$  close to 1 (since all vectors are normalized), we call the point a HT.

$$\mathbf{v}_i^u \cdot \mathbf{v}_i^s \geq \gamma \quad \implies \quad \mathbf{x}_i \text{ is located near a HT.} \quad (3.8)$$

In practice, we choose  $\gamma = 0.9999$ . The result for these parameters is shown in Figure 3.2. The four HTs around the x axis, with y values close to 0, are called primary homoclinic tangencies (PHTs) [18]. In principle, there is an infinite amount of HTs, since every image and every

---

<sup>2</sup>Since we start with an arbitrary vector  $\mathbf{v}_0^u$ , we discard the first 20 iterations, so that the components normal to the strongest expansion direction get sufficiently suppressed.

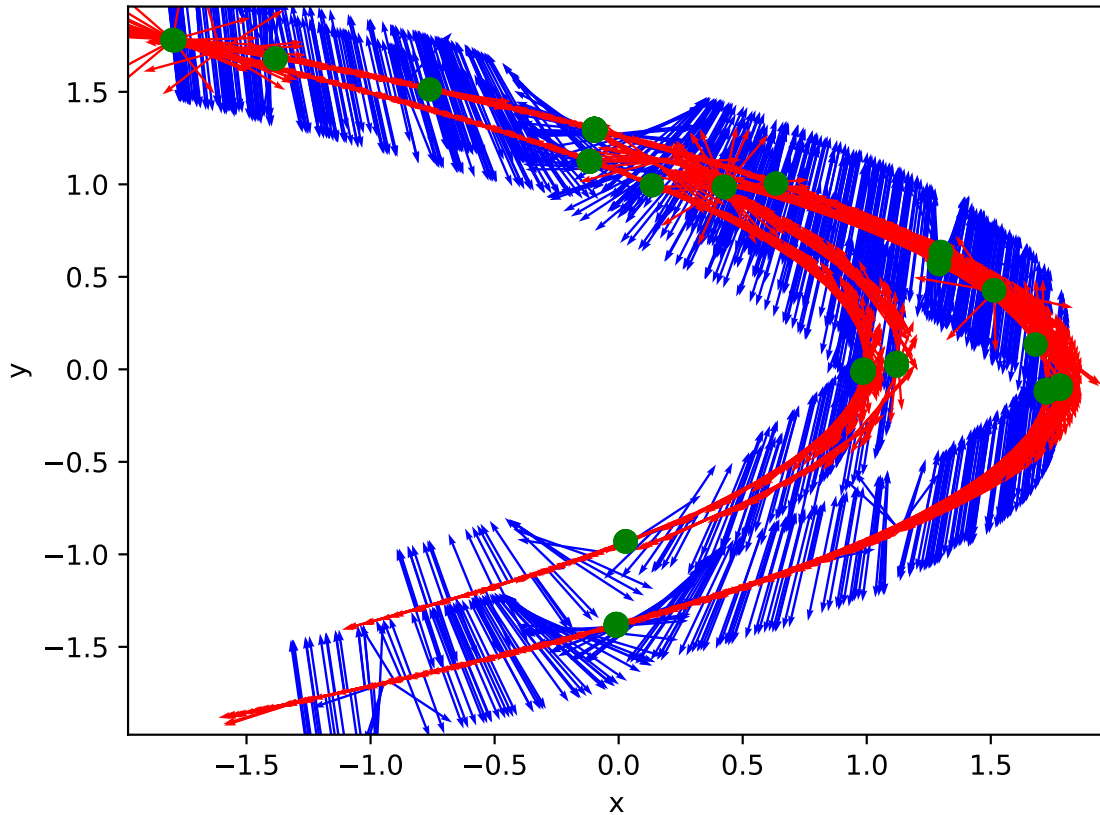


**Figure 3.2:** Unstable manifold (red), Stable manifold (blue) and HTs (green). Only every 50th of the calculated values is plotted, for better visualization. The arrows are scaled down from unity for the same reason.

preimage of a HT is again a HT. The primary HTs are defined by the fact that the sum of the curvatures of both manifolds is minimal [10]. Therefore, the PTHs have a bigger area in phase space around them, for which both manifolds are nearly tangential and where subsequently the effects of nonhyperbolicity are relevant. This area is called the critical region. HTs where the curvature of the manifolds is big (which applies for most HTs), have a very small critical region and do not exhibit many effects of nonhyperbolicity. In practice, only the HTs with a sufficiently big critical region are regarded and the rest of the attractor can be treated as if it were hyperbolic [10].

In the following segment we will see how the previously calculated UPOs connect to the presence of HTs on the attractor.



# 4 Effects of Nonhyperbolicity

The attractor of a dissipative map can be visualized by plotting a very long trajectory from a starting point inside the basin of attraction. For the Hénon map and the baker map, the respective attractors are shown in Figure 2.1. UPOs can be used to calculate the natural measure of a hyperbolic system [2] and, as strong evidence suggests, also of a nonhyperbolic system [14]. It is therefore a plausible guess that the distribution of UPOs of a nonhyperbolic system converge towards the natural measure, as it is the case for hyperbolic systems [8].

For short period lengths, nonetheless, we observe two major indicators that the above stated assumption is not actually valid: areas on the attractor with no periodic points at all and a systematic difference between the large-scale distribution of periodic points with respect to the natural measure.

Both phenomena will be investigated in this section.

## 4.1 Gaps around Homoclinic Tangencies

At several points on the Hénon attractor we observe regions which are void of periodic points. We will call these regions gaps. As we can see in Figure 4.1, they are located around homoclinic tangencies. The figure shows the primary generating partition, connecting the primary HTs and the first three backiterates of the primary generating partition. The intersections between these generating partitions (GPs) and the attractor mark the HTs with the biggest critical regions [10]. The effects of nonhyperbolicity are expected to be strong in these areas. Accordingly, we observe that the critical regions around the major HTs, crossed by the depicted GPs, exhibit the biggest gaps. We also observe that the HTs are always located in the center of a gap, with a seemingly symmetric behaviour of the periodic points around it.

To investigate how the occurrence and size of the gaps depends on the period length, we plot the UPOs for four different  $p$  in Figure 4.2. We see that the gaps close for higher period lengths. But the closing does not occur simultaneously in all HTs. Already for  $p = 16$  two of the PHTs do barely exhibit gaps around them and the gaps around the other two PHTs close for different  $p$  respectively.

To study the closing more quantitatively, we calculate the point density around the PHTs for different period lengths. We look at the amount of points located in different distances from the PHTs (see Figure 4.3), normalized with the amount of chaotic points in the same ring. The

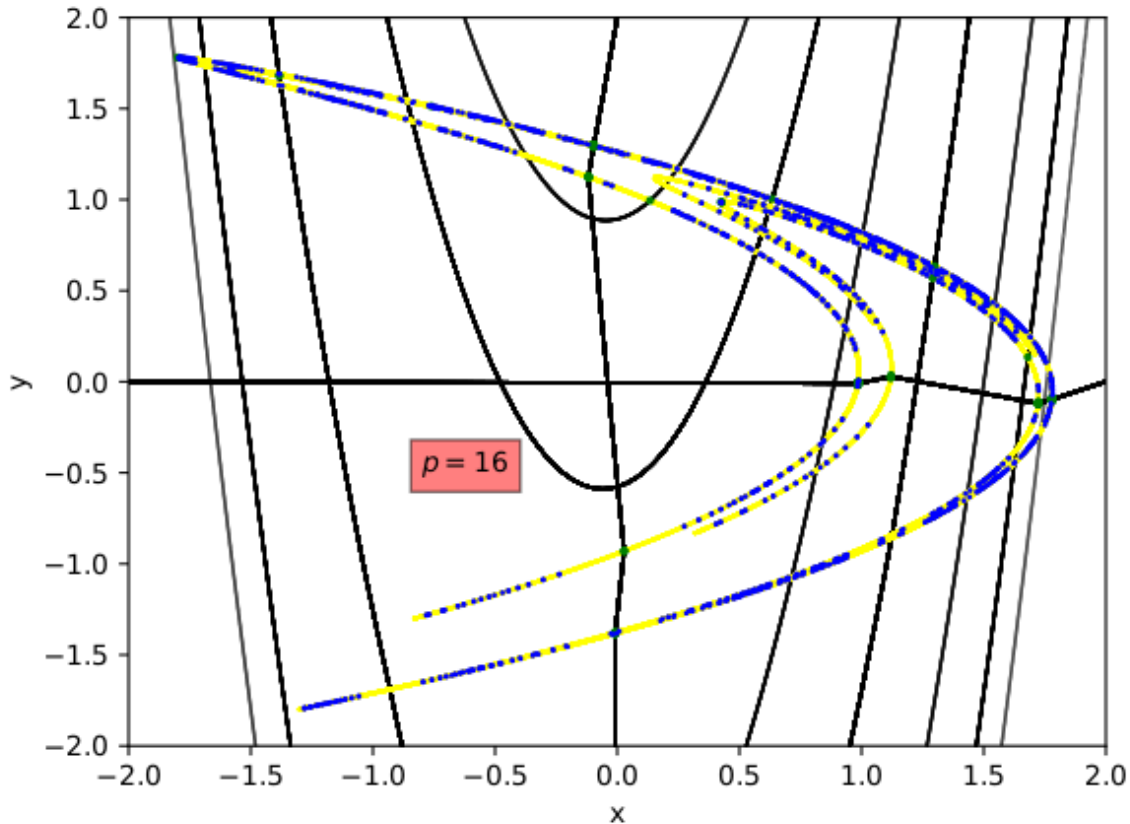


**Figure 4.1:** UPOs (blue), HTs (green) and attractor (yellow) together with the primary generating partition and its first three backiterates (black) for  $p = 16$ .

chaotic orbit that we use for normalization is of length  $N(p)$ , equal to the amount of periodic points in period  $p$ . For every  $p$ , the density  $D_r$  depending on the radius  $r$  is calculated by

$$D_r = \frac{\# \text{ periodic points in } R_r}{\# \text{ chaotic points in } R_r}, \quad (4.1)$$

where  $R_r$  is the ring with radius  $r$ .

For the two PHTs of Figure 4.3, the  $D_r$  are shown in Figure 4.4. We see that, generally, higher period UPOs get closer to the HTs. Lower period orbits have no points at all in the regarded areas around PHTs and the higher period orbits increasingly approach the HT, as in Figure 4.4(d). Yet this process of approximating the HT, of closing the gaps as  $p$  increases, is not monotonous. Sometimes, contrary to the general trend, periodic points from lower period UPOs lie closer to the HTP than some higher period UPOs, as we can see in Figure 4.4(c) for  $p = 16$ . Moreover, even high period UPOs with points in nearly every ring, have a density much lower than 1, which means that the periodic point density is lower than that of the chaotic trajectory used for normalization.

Still, since we have only UPO data up to a certain period length  $P = 21$ , it is conceivable that

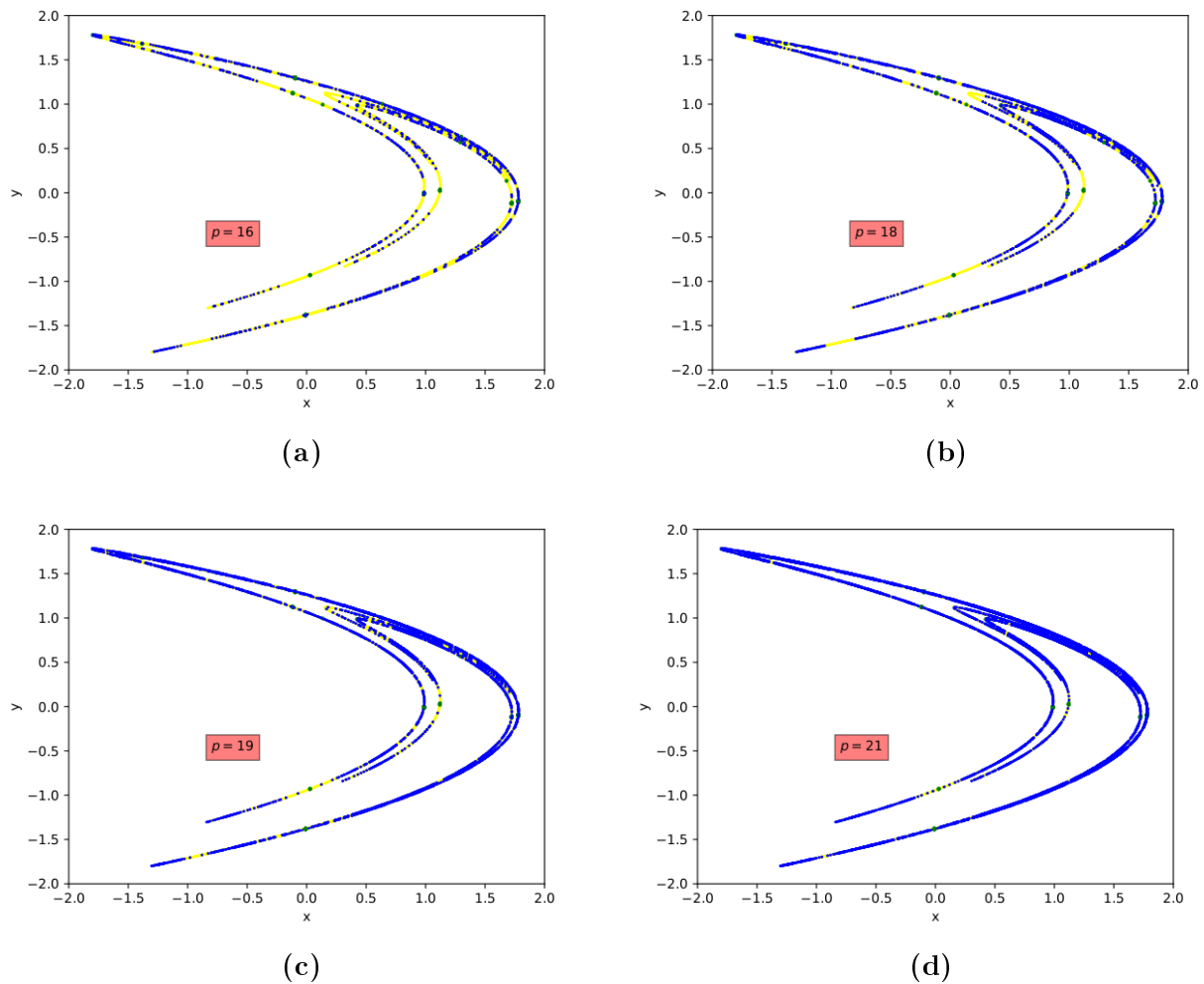


**Figure 4.2:** UPOs (blue), HTs (green) and attractor (yellow) for four different period lengths.

for  $p \rightarrow \infty$ , the gaps close completely and reach the same distribution as that of a long chaotic orbit, namely the natural measure. This hypothesis will be investigated further in section 4.2.

In order to determine whether the observed gaps are really a feature of nonhyperbolic systems, we compare UPOs with an approximation of the natural measure in the hyperbolic baker map. In Figure 4.5 we plotted the periodic points over the attractor for  $p = 12$  and  $p = 16$ . The whole attractor is covered by the UPOs, there are no apparent gaps. When randomly zooming into the fractal structure of the attractor, we see that the periodic points are distributed uniformly among the nonperiodic points. This is exactly what we expect, since we connected the existence of gaps to HTs, which are not present in a hyperbolic map. A more quantitative assessment of the relationship between UPOs and the attractor of the baker map is done in the following section.

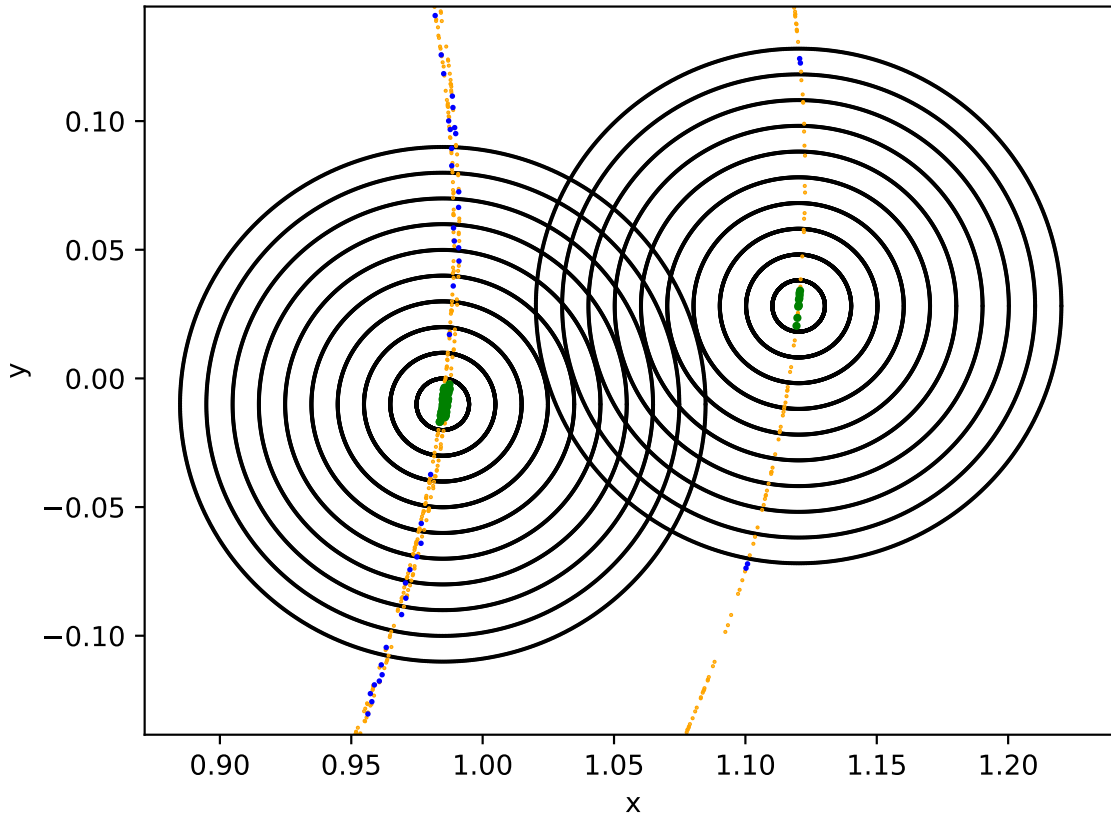


**Figure 4.3:** Concentric rings to evaluate point density around two PHTs (green) for different radii. UPOs (blue) and a chaotic orbit (orange) with the same total amount of points

## 4.2 Distribution of periodic points

From a broader perspective, it is interesting to ask whether UPOs have the same spatial distribution as the natural measure and how this depends on the hyperbolicity of the map.

This question is investigated by covering the phase space with quadratic boxes. For every box, the number of included periodic points is counted. As a comparison, a chaotic trajectory with a length  $N(p)$  equal to the amount of points of period  $p$  is evaluated in the same way. Additionally, we compute the natural measure by a long chaotic trajectory.<sup>1</sup> With this data, it is possible to compare the convergence of UPOs towards the natural measure with the convergence of a random chaotic orbit.

Since the previously discussed gaps on the attractor seem to diminish for longer period lengths of UPOs, a natural hypothesis is that they are a phenomenon only of short periodic orbits. For longer orbits, the gaps could asymptotically close, such that the distribution of periodic points would approximate the natural measure.

If this were the case, one would expect that both the chaotic and the periodic points approach

<sup>1</sup>The trajectory consists of  $10^5$  points, excluding the first 100 iterations.



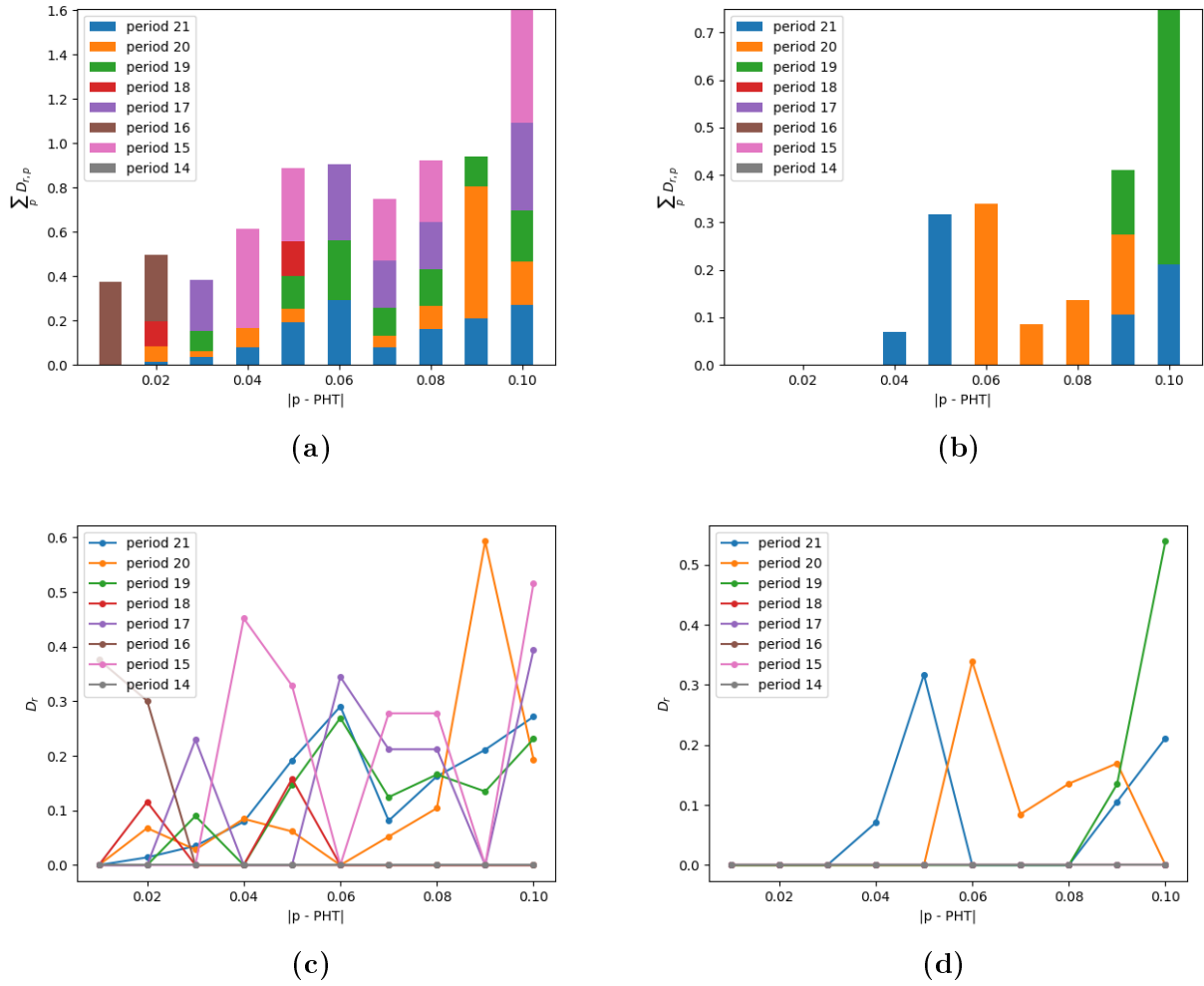


**Figure 4.4:** Density of periodic points  $D_r$  depending on radius  $r$ , which is calculated as the norm between a regarded point  $p$  and a PHT. (a) and (c) show the results for the PHT at (0.986, -0.009), (b) and (d) for the PHT at (1.12, 0.028).

the natural measure for higher period lengths. This hypothesis is examined by calculating the standard deviation of the difference between the amount of points per box for the two cases. Concretely, we choose a box size which determines the amount  $M$  of boxes per axis (for the Hénon attractor we choose a covering of  $([-2, 2], [-2, 2])$  with a box size of 0.08, which gives a grid of  $50 \times 50$  boxes). For every period, we obtain an  $M \times M$  matrix describing the distribution of periodic points (**A**), chaotic points (**B**) and the natural measure (**N**). Both **A** and **B** are compared to the natural measure by calculating the difference matrices  $\mathbf{D}_{\mathbf{AN}}$  and  $\mathbf{D}_{\mathbf{BN}}$ . Since the amount of points per period  $N(p)$  scales exponentially and we want to compare the results for different  $p$ , the difference matrices are divided by the number of total

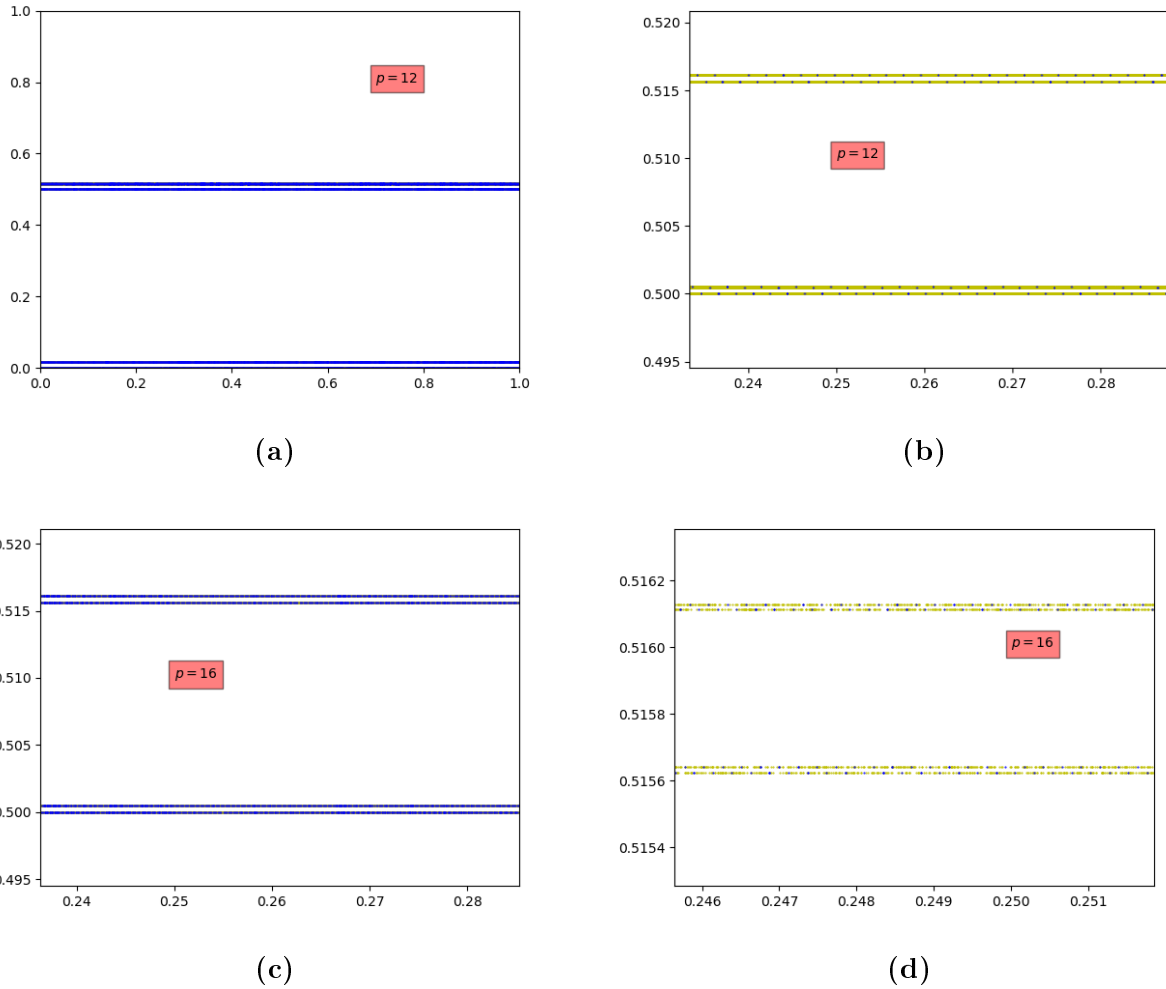


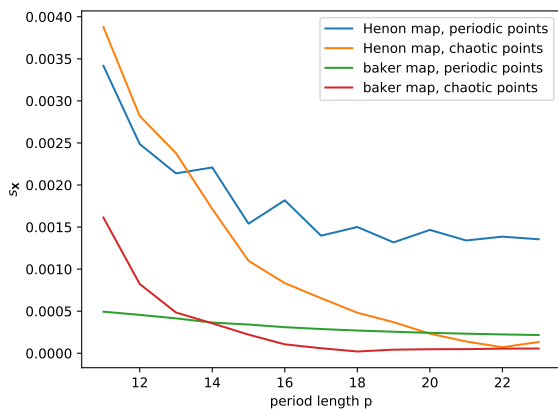
**Figure 4.5:** UPOs (blue) and attractor (yellow) of the baker map for two different period lengths.

points of this period.

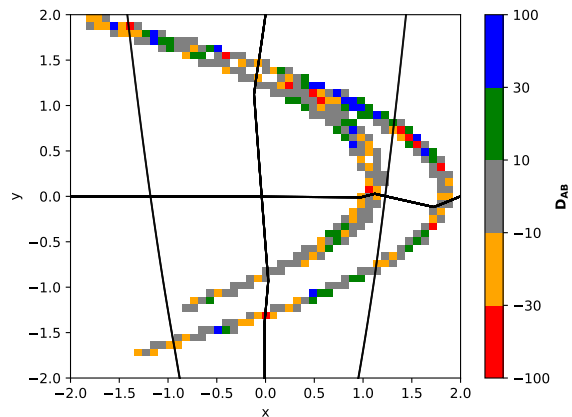
$$\mathbf{D}_{\mathbf{AN}} = \frac{1}{N(p)}(\mathbf{A} - \mathbf{N}), \quad \mathbf{D}_{\mathbf{BN}} = \frac{1}{N(p)}(\mathbf{B} - \mathbf{N}) \quad (4.2)$$

$\mathbf{D}_{\mathbf{AN}}$  and  $\mathbf{D}_{\mathbf{BN}}$  now contain the difference of the amount of points for every box. By calculating the standard deviation  $s_{\mathbf{X}} = \text{std}(\mathbf{D}_{\mathbf{XN}})$  for every value in  $\mathbf{D}_{\mathbf{AN}}$  and  $\mathbf{D}_{\mathbf{BN}}$  respectively, the deviation of the periodic points from the natural measure can be compared with that of the chaotic trajectory.

Figure 4.6(a) shows that for both maps the periodic and the chaotic trajectories differ significantly in their standard deviation (STD)  $s_{\mathbf{X}}$  of their difference matrices with respect to the natural measure. For the Hénon map, the STD of the chaotic orbit decreases fast, whereas the STD of the UPOs seems to reach a plateau at higher period lengths. The STD of the chaotic baker orbits seems to reach a lower limit, which is approached by the chaotic Hénon



(a) Standard deviations  $s_{\mathbf{X}}$  ( $X=A$  for periodic points and  $X=B$  for chaotic points) of the deviations of  $\mathbf{A}$  and  $\mathbf{B}$  from the natural measure  $\mathbf{N}$ . Shown for both maps.



(b) Differences  $\mathbf{D}_{\mathbf{AB}}$  per box between periodic and chaotic points of the Hénon map for two orbits of the same length ( $p = 19$ ). Three generating partitions to illustrate important HTs are included.

**Figure 4.6:** Deviation of the periodic points from the natural measure, quantitatively in (a) and qualitatively in (b).

orbits and, more slowly, by the periodic orbits of the baker map. Since the baker map has more points per period lengths (every possible binary sequence yields an existing orbit), it is clear that the magnitude of the STD is smaller than in the Hénon case.

Dividing the causes of the deviations from the natural measure into statistic and systematic factors, we conclude the existence of a systematic cause that prevents the periodic Hénon points from approaching the natural measure. Although the behaviour of periodic and chaotic points differs for the baker map as well, the difference is not as drastic as in the Hénon case and seems to decline for higher period lengths<sup>2</sup>. We therefore suspect that the high deviation for periodic points is an effect of the Hénon map being nonhyperbolic. It seems to be the case that, in a nonhyperbolic system, the distribution of periodic points does only approach the natural measure up to a certain point.

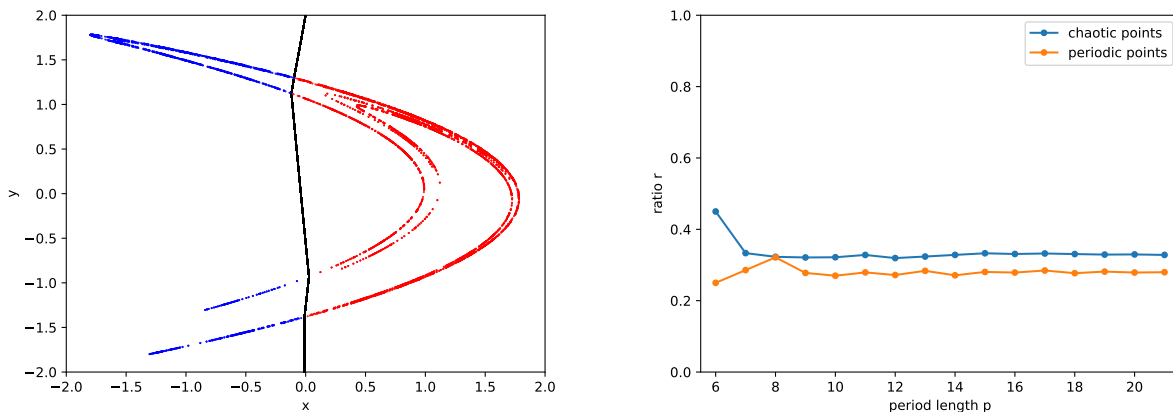
More precisely, a look at the spatial distribution of the differences makes clear that areas around HTs still exhibit a lower density of periodic points than a chaotic trajectory. Figure 4.6(b) shows the difference values for every box at  $p = 19$ . Negative values correspond to fewer periodic than chaotic points. The areas around HTs (e.g. the points where generating partitions intersect the attractor) mostly lie in and around boxes with a low density of periodic points. So, even if the apparent gaps get closed for higher period lengths, there does remain

<sup>2</sup>The data for the baker map is not as reliable as for the Hénon map, since the strong contraction in  $y$  direction leads to an extremely high sensitivity on the initial conditions. Floating point calculations yield significant numerical errors. We therefore work with the data type Decimal with 44 digits. Thereby we are able to reproduce the expected attractor, but we cannot fully exclude further numerical artifacts for long trajectories, such as round-off-induced periodicity.

a quantitative difference in the spatial distribution between the natural measure and periodic points<sup>3</sup>.

Having a broader look at the distribution of points on the nonhyperbolic Hénon attractor, it is sensible to analyze the symbolic dynamics of orbits. This is equivalent to analyzing how many points lie on which of the two binary partition elements. For the periodic points of the Hénon map, this is easily done, since the constant factor  $s_n$  used in the Biham-Wenzel algorithm corresponds to the location of the point with respect to a generating partition (see Figure 4.7(a) or [11]). It is therefore sufficient to calculate the amount of points coded with a 1 and a 0 respectively, named  $n_1$  and  $n_0$ . Doing this separately for every period length, we see in Figure 4.7(b) that the proportion of points coded with 1 approaches the value  $r = 0.279$ . This ratio  $r$  is defined by

$$r = \frac{n_1}{n_1 + n_0}, \quad n_1 + n_0 = N(p), \quad (4.3)$$



(a) UPOs of  $p = 19$  with generating partition. Blue points correspond to symbol 1, red points to 0 in the symbolic dynamics.

(b) Share of total points coded with symbol 1, for periodic and chaotic points. Calculated for different period lengths  $p$ .

**Figure 4.7:** Separation of points based on their symbolic dynamics and distribution of symbols for the periodic and nonperiodic case.

To get the distribution of the natural measure, we let a chaotic trajectory run for many iterations and count how many points fall on which partition element respectively. If the UPOs were to approximate the natural measure, one would expect the same result as for the periodic points. Yet the resulting value is  $r = 0.327$ .<sup>4</sup>

<sup>3</sup>The amount of points at  $p = 19$  is  $L = 18549$ . There are 291 non-empty boxes in phase space, which leads to an average of 63.7 points per boxes. The fact that many boxes have differences of more than 30 points, emphasizes the magnitude of the deviations.

<sup>4</sup>This value was calculated with  $10^8$  iterations.

---

Figure 4.7(b) shows the ratios  $r$  for both the periodic and the chaotic points for different period lengths, always regarding the same amount of points per period. The ratio indicates the spatial location of points on the attractor. It is evident that the distribution of points with respect to generating partitions is systematically different between UPOs and chaotic orbits. As this imbalance must hold with respect to any possible generating partition, this means particularly that points concentrate on the upper right half of the attractor (regarding the primary generating partition and its first backiterate). Looking at Figure 4.6(b) we see that this quadrant does indeed seem to exhibit a higher concentration of periodic points, marked with green and blue colours.

We conclude that, given the constant imbalance of the macroscopic distribution of UPOs with respect to the natural measure, they do not approach the natural measure for higher period lengths. This systematic difference between UPOs and the natural measure is surprising, but it could help to find an explanation for the origin and cause of the previously observed gaps.

### 4.3 Origin of gaps in the Hénon attractor

We saw in section 4.1 that the observed gaps on the Hénon attractor form around points of homoclinic tangencies. Having seen in section 4.2 that even for higher period lengths the areas around HTs have a lower density of periodic points with respect to the natural measure, the question arises, whether there is a mechanism driving UPOs away from HTs.

The claim of this thesis is that the formation as well as the closing of the gaps on the attractor can be understood on the basis of symbolic dynamics and generating partitions.

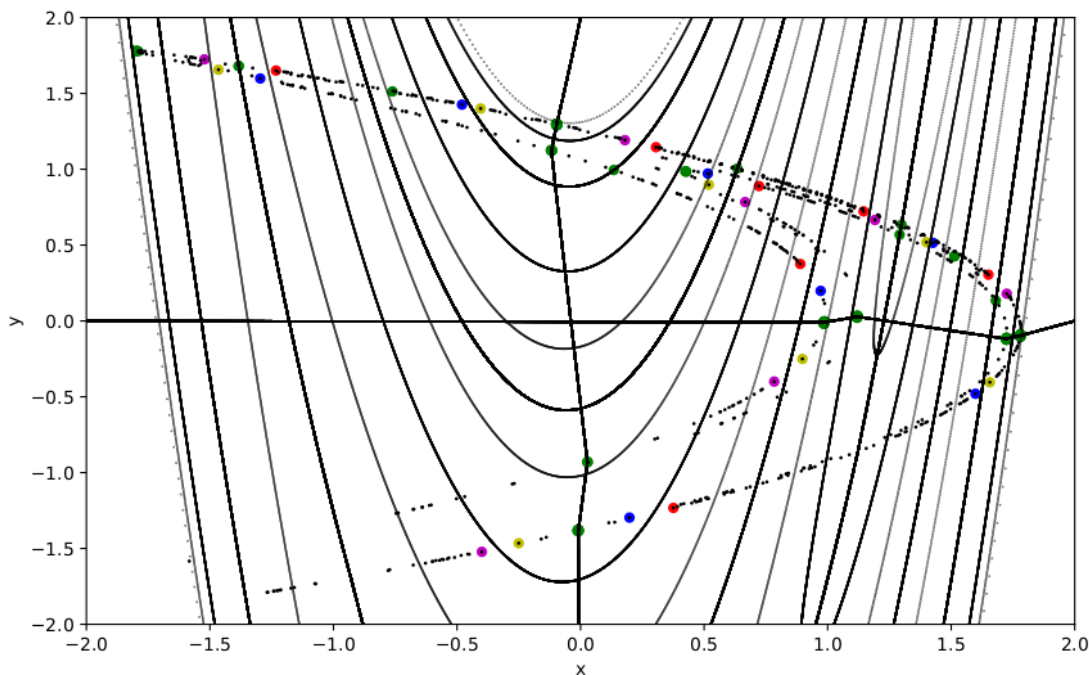


**Figure 4.8:** Periodic points of period  $p \leq 12$  and the primary GP with its first 6 backiterates. The UPOs of  $p = 7$  are highlighted in colour and the HTs are marked in green.

There are four different orbits of period seven, as depicted in Figure 4.8. Several aspects are noticeable in this plot. For one, the four orbits are always symmetrically allocated around a HT. Secondly, there are always two points on either side of the HT, but in varying combinations. Apparently, all four orbits show a surprisingly similar trajectory in phase space. Not only do they all lie around the same HTs, they also iterate from one HT to the next in the same order. The difference between the four orbits is encoded in the fact, on which side of the HT, i.e. in which partition element, the points lie.

This can be better understood when looking at the symbolic dynamics of the period seven orbits, as shown in Table 4.1. A point is coded with a 1 if it lies in the lower and with a 0 if it lies in the upper partition element (with respect to the primary partition line<sup>5</sup>). The four

<sup>5</sup>All the following explanations are equally valid with respect to any other of the seven partition lines. For the

**Table 4.1:** Symbol sequences for the length  $p = 7$  UPOs

symbol sequence	colour in Figure 4.8
(0000001)	red
(1000001)	pink
(0000101)	blue
(1000101)	yellow

symbol sequences differ only in two of the seven digits. The two digits where two sequences are 1 and two are 0 represent the points around the primary HTs, since in both cases two points lie above and two points lie below the partition line. The last digit, which is 1 for all four orbits, represents the points around the HT at  $\approx (0.0, -1.4)$ , since all four points lie in the lower partition element.

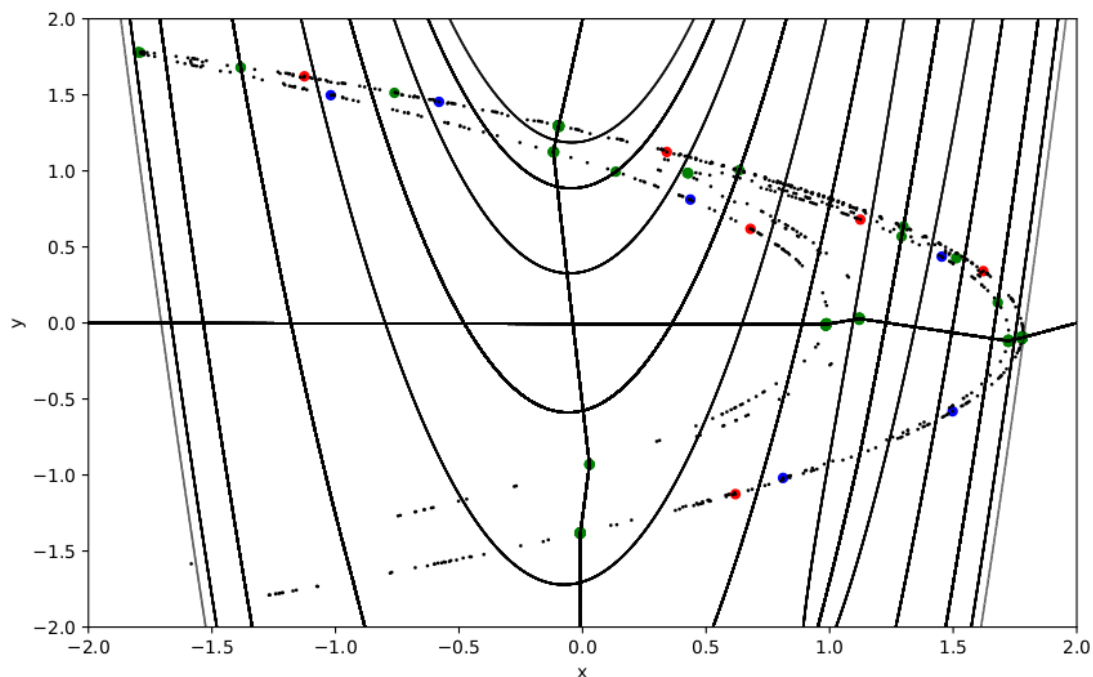


**Figure 4.9:** Periodic points of period  $p \leq 12$  and the primary GP with its first 5 backiterates. The UPOs of  $p = 6$  are highlighted in colour and the HTs are marked in green.

The mechanism responsible for the symmetry around HTs appears to be the following: Consider two symbol sequences of length  $p$  differing in only one digit. This implies that they must lie in the same partition element during all iterations except for one. Since generating parti-

---

vertical line, 1 would code the left side and 0 the right side. The others have a more complicated structure, but the same properties.

**Table 4.2:** Symbol sequences for the length  $p = 6$  UPOs

symbol sequence	colour in Figure 4.9
(000001)	red
(000101)	blue

tions are constructed through the connection of HTs<sup>6</sup>, and since all preimages of a generating partition are again generating, the two orbits must be distinguishable with respect to any of the  $p$  different partitions. Therefore, for every iteration the two points have to be separated by a generating partition and thus lie on different sides of a HT. In fact, the Figures 4.8 and 4.9 both show, that  $p$  different generating partitions together divide the phase space in such a way that every periodic point of this period lies in a different partition element. The period six orbits of Figure 4.9 show how two points of different orbits are always separated by a generating partition and enclose a HT<sup>7</sup> at every iteration, given that they have a similar symbolic dynamics.

Comparing the period six with the period seven UPOs in Tables 4.2 and 4.1, it is striking how similar the symbolic dynamics of the existing orbits are for both periods. The difference for the orbits drawn in red and blue (Figure 4.8 and 4.9) consists in one added 0 only. The resulting dynamics is similar, but not completely analogous. The HTs that are enclosed by the pair of points show significant differences, comparing period six and period seven orbits. Figure 4.8 shows all periodic points up to period length  $p = 12$ . Looking closely, it is evident that the period six and seven orbits are not a special case, but prime examples of a general phenomenon. Around many of the HTs, the periodic points are distributed symmetrically to both sides (see Figure 4.2).

This phenomenon allows a simple explanation for the origin of the gaps discussed in section 4.1. The allowed symbolic sequences for UPOs of a given length  $p$  are similar. The symbol 0 dominates the symbolic dynamics. As we saw earlier in section 4.2, the abundance of 0 is nearly constant for all periods (see Figure 4.7). Almost three out of four symbols are a 0. Together with the exclusion of cyclic permutations, this automatically leads to similar symbolic dynamics and thereby to orbits having similar dynamics throughout phase space, while always being separated by a generating partition and thus a HT. For longer period lengths  $p$ , the phase space is subdivided into smaller cells by the primary partition and its  $p - 1$  preimages. Therefore, for higher period lengths, in order to still be separable, the points must lie closer to each other and to the HT. This leads to the observed effect of the gaps closing for higher  $p$ . Earlier we discussed the concept of critical regions around HTs and stated that those with the

<sup>6</sup>For more details see [25].

<sup>7</sup>Not all HTs are drawn in green in Figure 4.9. This is due to the chosen threshold value  $\gamma$  in 3.3. But even if no green dot is drawn, the crossing of the attractor with a generating partition is equivalent to the presence of a HT.



---

biggest critical regions are the primary HTs and their lowest iterates. In Figure 4.9 we see that the partition elements containing the longest segments of the attractor lie next to these HTs with the biggest critical regions. It is well visible that the partition elements around  $(0, -1)$ ,  $(0, 1.3)$  or  $(1, 0)$  have a noticeably low density of periodic points. We conclude that the regions around strong HTs, where thus the effect of the nonhyperbolicity is strong, have neighbouring partition elements which enclose an especially big part of the attractor. This explains why the regions around strong HTs exhibit a considerably lower density of UPOs with respect to the natural measure. Given a partition element containing a big segment of the attractor, the overall density of periodic points is smaller than in a narrow segment, containing only a small part of the attractor. This hypothesis is supported by the fact that the boxes with fewest periodic points in Figure 4.6(b) coincide with the biggest partition elements in Figure 4.9, whereas the boxes with most periodic points are located in the upper right half of phase space, where it is subdivided into particularly fine segments.

Observing that, because of the parabolic shape of the higher iterate generating partitions, the upper half of the attractor is generally divided into more segments than the lower half, the question arises, whether this might actually be the cause for the abundance of periodic points in this partition element. This hypothesis is worth to be examined in further research.

Periodic points of different orbits are always separated by a generating partition, therefore they always lie on different sides of a homoclinic tangency: We conclude that the framework of generating partitions facilitates such a concise formulation of the mechanism that can explain the formation and the closing of the gaps on the Hénon attractor as well as the macroscopic deviations of UPOs from the natural measure.



# 5 Summary and Outlook

To investigate the effects of nonhyperbolicity on the dynamics of two-dimensional dynamical systems, we focused on the nonhyperbolic Hénon map and on the hyperbolic baker map. This thesis is especially about the effects that the nonhyperbolicity has on unstable periodic orbits and their distribution in phase space.

After briefly introducing the theoretical foundations in Chapter 2, Chapter 3 was dedicated to describe the numerical calculations. We calculated the UPOs for both systems, as well as the points of homoclinic tangencies for the Hénon map. This data could then be used to start the analysis of the periodic points on the attractor and investigate how the nonhyperbolicity affects the location of periodic points.

We saw in Chapter 4 that, qualitatively, there is an interesting phenomenon occurring in the nonhyperbolic Hénon map. Around the major HTs, there are regions with no periodic points for low period lengths, and these gaps fill up for higher period UPOs. We calculated the relative density of periodic points with respect to nonperiodic points in different distances from the HTs for all period lengths. This confirmed our observation, that points of higher period length get increasingly closer to the HTs, thereby leading to the effect of the gaps closing. At the same time, we saw that this process does not occur in a regular manner. The period length at which the closing occurs and the speed of it is very variable. Some HTs even have outliers, for which smaller period UPOs lie significantly closer to the HTs than higher period UPOs. We conclude that the effect of gaps closing for higher period lengths does exist, but it is not an easy and smooth process of decreasing repulsion from the HTs, but the consequence of a more systematic imbalance in the nonhyperbolic system.

By analyzing the general distribution of periodic points in phase space, we saw that there is a significant difference in location between UPOs and a long chaotic orbit approximating the natural measure. There are regions with a substantially higher share of periodic points and, around HTs, regions with fewer periodic points. Analyzing the difference between a periodic and a nonperiodic orbit approaching the natural measure, we saw that the periodic orbits retain a substantial deviation from the natural measure, which is not present in the nonperiodic case and seems to be constant for all higher period lengths.

Additionally, we noted that the distribution of points with respect to generating partitions differs between periodic and nonperiodic orbits. Both cases exhibit a rate between the two partition elements which is nearly constant for all lengths, but significantly different.

The results of this work clearly state that the nonhyperbolicity of a map with HTs leads to many effects that are not present in the hyperbolic case, such as regions of the attractor with almost no periodic points. We claim that the formation of these gaps can be understood with the concepts of symbolic dynamics and generating partitions. An explanation is outlined, which allows to see the gaps around HTs as a necessary consequence of the fact that periodic orbits have to be separated by every possible generating partition. Combining this with the similarity of the existing symbolic dynamics, we can understand the symmetric allocation of periodic points around HTs and even the closing of the gaps for higher period lengths.

It is thus interesting to invest further research into the origin of the similar symbolic dynamics. The imbalance with respect to generating partitions that we noted earlier, could indicate a route for further investigation. To examine the connection between this imbalance and the nonhyperbolicity of the dynamical system, it is necessary to analyze this distribution for more hyperbolic and nonhyperbolic systems.

The generality of the proposed explanation for the formation of gaps on the Hénon attractor could be checked by examining nonhyperbolic systems with a more balanced distribution of points between the two elements of a generating partition. It is an open question if such a system would still have UPOs with such similar symbolic dynamics. This would shed more light on whether the symmetrical gaps around HTs are an effect restricted to the Hénon map or whether it is a general feature of nonhyperbolic dynamical systems.

## 6 Bibliography

- [1] H. G. Schuster and W. Just. *Deterministic Chaos: An Introduction*. Wiley-VCH, Weinheim, 4., rev. and enl. ed. edition, 2005.
- [2] E. Ott. *Chaos in dynamical systems*. Cambridge Univ. Pr., Cambridge :, 1. publ. edition, 1993.
- [3] P. Grassberger and I. Procaccia. Measuring Strangeness in Strange Attractors. *Physica D: Nonlinear Phenomena*, 9:189–208, 10 1983.
- [4] E. Ott. Attractor dimensions. *Scholarpedia*, 3(3):2110, 2008. revision #91015.
- [5] A. Katok. Lyapunov exponents, entropy and periodic orbits for diffeomorphisms. *Publications Mathématiques de l’IHÉS*, 51:137–173, 1980.
- [6] J.-P. Eckmann and D. Ruelle. *Ergodic theory of chaos and strange attractors*, pages 617 – 653. Springer New York, New York, NY, 2004.
- [7] A. Politi. Lyapunov exponent. *Scholarpedia*, 8(3):2722, 2013. revision #137286.
- [8] R. Bowen. Periodic Points and Measures for Axiom A Diffeomorphisms. *Transactions of the American Mathematical Society*, 154:377–397, 1971.
- [9] A. Katok and B. Hasselblatt. *Introduction to the Modern Theory of Dynamical Systems*. Encyclopedia of Mathematics and its Applications. Cambridge University Press, 1995.
- [10] L. Jaeger and H. Kantz. Homoclinic tangencies and non-normal Jacobians — Effects of noise in nonhyperbolic chaotic systems. *Physica D: Nonlinear Phenomena*, 105:79–96, 06 1997.
- [11] P. Grassberger, H. Kantz, and U. Moenig. On the symbolic dynamics of the Henon map. *Journal of Physics A: Mathematical and General*, 22(24):5217–5230, dec 1989.
- [12] P. Cvitanović, G. H. Gunaratne, and I. Procaccia. Topological and metric properties of Henon-type strange attractors. *Physical Reviews A*, 38:1503–1520, 08 1988.
- [13] K. Gelfert and H. Kantz. Dynamical quantities and their numerical analysis by saddle periodic orbits. *Physica D: Nonlinear Phenomena*, 232:166–172, 08 2007.

- 
- [14] Y.-C. Lai, Y. Nagai, and C. Grebogi. Characterization of the natural measure by unstable periodic orbits in chaotic attractors. *Physical Review Letters*, 79(4):649–652, 1997.
- [15] P. Cvitanović and R. Mainieri. *Chaos: Classical and Quantum*. Niels Bohr Institute, Copenhagen, [ChaosBook.org](http://ChaosBook.org), 2016.
- [16] J. Meiss. Dynamical systems. *Scholarpedia*, 2(2):1629, 2007. revision #137210.
- [17] S. Smale. Differentiable Dynamical Systems. *Bull. Am. Math. Soc.*, 73:747, 01 1967.
- [18] P. Grassberger and H. Kantz. Generating partitions for the dissipative Hénon map. *Physics Letters A*, 113:235–238, 12 1985.
- [19] Y. Sinai. Kolmogorov-Sinai entropy. *Scholarpedia*, 4(3):2034, 2009. revision #91407.
- [20] M. Hénon. A two-dimensional mapping with a strange attractor. *Comm. Math. Phys.*, 50(1):69–77, 1976.
- [21] H. Wen. A review of the Hénon map and its physical interpretations. *Sch. Phys. Georg. Inst. Technol. Atlanta, GA 30332-0430*, pages 1–9, 2014.
- [22] C. Grebogi, E. Ott, and J. A. Yorke. Unstable periodic orbits and the dimensions of multifractal chaotic attractors. *Physical review. A*, 37:1711–1724, 04 1988.
- [23] O. Biham and W. Wenzel. Characterization of unstable periodic orbits in chaotic attractors and repellers. *Physical review letters*, 63:819–822, 09 1989.
- [24] O. Biham and W. Wenzel. Unstable periodic orbits and the symbolic dynamics of the complex hénon map. *Physical review. A*, 42:4639–4646, 11 1990.
- [25] L. Jaeger and H. Kantz. Structure of generating partitions for two-dimensional maps. *J. Phys. A: Math. Gen*, 3097:567–576, 08 1997.

## **Erklärung**

Hiermit erkläre ich, dass ich diese Arbeit im Rahmen der Betreuung am Max-Planck-Institut für Physik komplexer Systeme ohne unzulässige Hilfe Dritter verfasst und alle Quellen als solche gekennzeichnet habe.

Felix Schaumann

Dresden, 04. Juni 2019